

Novel Delayed Poincaré's Plot Indices of Photoplethysmogram for Classification of Physical Activities

Zahra BARATI MOGHADAM, Masoumeh SEPEHRI NOGHONDAR and Ateke GOSHVARPOUR*

Department of Biomedical Engineering, Imam Reza International University, Rezvan Campus (Female Students), Phalestine Sq., Mashhad, Razavi Khorasan, Iran

E-mails: m44b.moghadam@gmail.com; m.sepehri1376@gmail.com;

ateke.goshvarpour@gmail.com; ak_goshvarpour@imamreza.ac.ir

* Author to whom correspondence should be addressed; Tel.: +98-51-38041 (Ext. 3131)

Received: 7 January 2021 / Accepted: 23 March 2021/ Published online: March 30, 2021

Abstract

Purpose: Today, with the advancement of engineering sciences and technology in sports and physical health, the monitoring of physical activity has become the focus of many researchers. Accordingly, in this study, a new method has been proposed for classifying different sports activities based on the Photoplethysmogram signals. *Methods:* Four exercise activities, including running, walking, and cycling in light and heavy conditions, were used in this study. Data from the physionet database were used to perform the research, which included eight healthy participants with a mean age of 26.5. New criteria have been introduced for signal analysis based on the asymmetry of the delayed Poincaré's plots. *Results:* The Wilcoxon statistical analysis results showed a significant difference between different sports activities ($p < 0.05$). A support vector machine was implemented for classification. To this effect, we have adopted a one vs all strategy. According to the classification results, the highest performance was related to walking detection, where the accuracy of 80.17%, the sensitivity of 81%, and the specificity of 75% were achieved. *Conclusion:* In summary, new indicators of delayed Poincaré's plot can be effectively used to improve assessments of exercise activities or in designing personalized exercise programs.

Keywords: Photoplethysmogram; Delayed Poincaré's Plot; Asymmetry; Classification; Support Vector Machine

Introduction

The undeniable impact of the body and the psyche on each other has made any body or mind experience affect the whole organism and body system. The ability to perform sports depends on the performance and function of different body systems. It can be said that planned exercise and physical activity will enhance and improve various body systems such as the cardio-respiratory system and improve physical fitness. Exercise is one of the simplest, safest, cheapest, and most natural ways to deal with physical and mental problems [1].

Today, thanks to the advances in technology in sports and physical health, the monitoring of physical activity and participants' health have become the focus of many researchers. For this

purpose, the monitoring process can be performed using various signals such as an electrocardiogram (ECG), heart rate (HR), and photoplethysmogram (PPG). Photoplethysmography is an optical measurement method used to detect blood volume changes in the microvascular tissue substrate. This process is accomplished by shedding light on body parts and measuring the amount of reflected light. It is acquired noninvasively. The signal obtained by this method is one of the simplest signals in the way of data collection during exercise that can monitor the activity of the heart [2]. Previously, for monitoring body activity during exercise, most researchers have examined cardiac functions. The results of Hosseini et al. indicated an increase in heart rate and mean arterial blood flow during exercise and physical activity [2, 3]. In another study, Zali et al. stated that in general, in all disorders caused by sympathetic and parasympathetic imbalances, cardiac analysis can accurately provide information about changes in the autonomic system function [2]. Almost the majority of scientific evidence and research findings suggested that regular physical activity can prevent various physical, mental, and mental illnesses [1]. This regular exercise program is beneficial for the health and recovery of other disorders. Piralaiy et al. concluded that moderate-intensity aerobic exercise could improve cardiac rhythm and ultimately increase heart rate variability in diabetic patients with peripheral neuropathy by improving cardiac autonomic function [4]. Kayhani and her colleagues showed that a proper exercise rehabilitation program would improve patients' mental status and quality of life with heart failure [5]. Shirzadi et al. established that in addition to the physical benefits of exercise, it is also effective in treating depression [6]. Precisely, their study indicated that exercise promotes vitality and reduces depression. In another experiment, it was determined that myocardial infarction is 6% less common among athletes than non-athletes [7].

Goa et al. proposed a framework for exercise monitoring. They have presented an XGBoost-based fitness assessment model using advanced feature selection and Bayesian parameter optimization. The authors concluded that the best way to monitor cardiac function during physical activity is to use smart bands that worked based on PPG signals [7]. In a study, Mobinuddin Ahmed and his colleagues reported that although accelerometers are used to measure physical activity, they have some problems. They could not provide complete information about the biomedical signal. Consequently, classifying and identifying physical activity is not an easy task simply by using one simple rule or any general rule. As a result, the program requires a machine-learning algorithm that can detect a person's physical activity based on the pulse rate data [8].

The effect of endurance training on autonomic cardiac control was studied by Carter et al. [9]. In this regard, some spectral and statistical approaches, as well as the effect of gender and age was assessed. The results highlighted higher parasympathetic and lower sympathetic activity at rest as a result of endurance training. In addition, the role of physiological aging on parasympathetic reduction and gender-wise autonomic control of heart rate was revealed. Lewis and Short [10] attempted to quantify between-lead agreement for QT at rest and during physical exercise. Their findings implicated differences in QT interval determined from multi-lead ECGs of the two groups. Lai et al. [11] studied the HRV in concussed athletes five days and two weeks after postinsult. A 5-minute ECG signal was recorded at rest and after biking. Precisely, the subject was imposed to a workload whilst maintaining a heart rate of 100 beats/min. After 15 minutes in this situation, the ECG was collected. The signals were characterized by mean RR interval and SDRR, LF power, HF power, total power, and approximate entropy (ApEn). Their results showed higher LF power, LF/HF, SDRR, and total power, as well as lower HF power and ApEn at 5 days. One of the limitations of this study was the case analysis of HRV. In addition, no signal changes were reported during the onset of the injury. Ciucurel et al. [12] proposed a new synthetic indicator to quantify the repetition of fractals in ECG at rest and during effort testing. Their results showed very strong correlations between the proposed measure and the heart rate values at rest and post-exercise. Although a new model has been proposed for quantifying ECG dynamics, the variability of the parameters during signal recording was ignored for fractal modeling. Wang et al. [13] endeavored to measure the fluctuations of Gaussian modeling features derived from finger PPG pulses during exercise and recovery. During the performance of different exercise loads (0, 50, 75, 100, 125W), as well as during the recovery period, the PPG pulses were recorded and normalized. Then, the signals were decomposed into three independent Gaussian waves. Next, the peak amplitude, peak time locus, mid-extent from each Gaussian trend, the peak time interval, and amplitude ratio between 1st, and 2nd, 3rd Gaussian waves

were extracted. Finally, they were compared between effort loads and recovery phases. The study concluded that there are significant changes in Gaussian modeling attributes with exercise and recovery. However, the irreversibility of the parameters to the baseline level over time indicated that the proposed properties should be validated and evaluated on the long-term PPG signal. Recently, Kuppusamy et al. [14] evaluated the effects of a yoga practice (Bhramari pranayama) on the HRV measures of healthy young adults. The yoga practitioners were asked to perform the exercise five days a week for a duration of six months. In contrast, the control group performed their daily routine. The short-term HRV signals were characterized using the following measures. The square root of the mean squared differences of successive NN intervals (RMSSD), the standard deviation of the NN interval (SDNN), the number of interval differences of successive NN intervals greater than 50 ms (NN50), and the division of NN50 by the total number of NN intervals (pNN50), normalized low frequency (LF nu), normalized high frequency (HF nu), and LF/ HF ratio. Their results showed that after 6 months of yoga breathing practice, a positive shift is observed in cardiac autonomic modulation towards parasympathetic predominance. Although the study was conducted in a community with a good number of samples, its focus was on practicing the breathing pattern of individuals during yoga, not specific physical activity. In addition, some statistical and spectral measures were used to analyze the short-term cardiac signal and did not evaluate the dynamics of the cardiac signal.

Most studies in this field have focused on ECG and HRV signals. Other researchers examined the PPG signal has been mainly tended to extract the HR from PPG, and its quantifications [15]. In this regard, the PPG dynamics, especially the PPGs phase space's geometry, have not been studied so far.

The advancement of technology in sports and the importance of physical health and physical activity are considered topics of interest among scientists. Therefore, the present study's purpose was to classify exercise activities using changes in the PPG signals. We investigated the PPG signals in four different sports conditions, including walking and running on a treadmill, cycling at low and high speeds.

Material and Method

We presented new criteria for delayed Poincaré's plots utilizing PPG signals to emphasize phase space dynamics. The extraction of new features was based on the asymmetry of the PPG signals' delayed phase space. Finally, by classifying the sports activities, the results of the analysis are discussed. Figure 1 illustrates the general process of the research method.

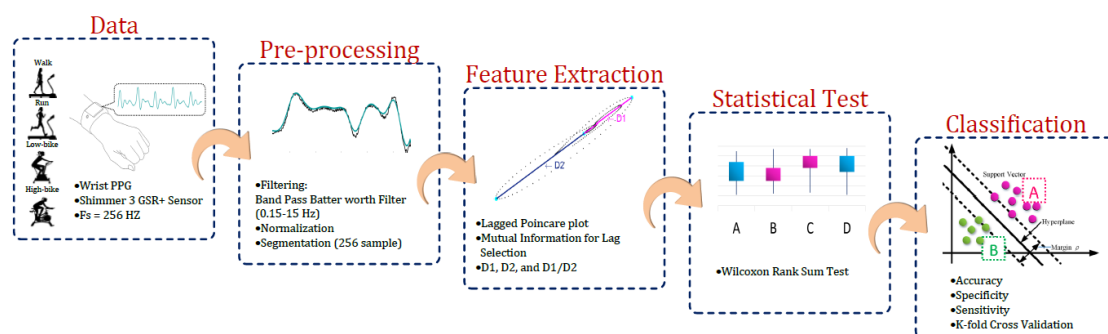


Figure 1. Diagram of the research process

Data

In the present study, the photoplethysmogram signals of eight participants were used, including 3 males and 5 females in the age range of 22 to 32 years and an average age of 26.5 years [16]. The signals are freely available at physionet databank. The database provides PPG signals simultaneously

with ECG signals of individuals. In this study, only the PPG signal was used for further analysis and processing. The PPG signals were recorded by a 3 GSR + shimmer with a sampling frequency of 256 Hz. The sensor incorporated a gyroscope, a low-noise accelerometer, and a wide-range accelerometer. Changes in blood oxygen content can be observed by closing the sensor to the wrist and radiating the light and then its reflection. These signals were recorded in four different modes of treadmill walking and running and low/high resistance cycling using a stationary bicycle. Subjects were asked to determine the timing and speed of walking and running and the rate of pedaling in cycling according to their ability. Table 1 shows the different data recording modes, the number of participants, and the data recording time.

Table 1. Duration of each activity (in MM:SS) by participants

Subject	Walk State	Run State	Low-Resistance Bicycle	High-Resistance Bicycle
1	9:4	-	9:39	9:48
2	6:39	-	5:41	6:54
3	4:47	5:07	4:54	4:41
4	-	4:52	-	-
5	-	5:08	4:40	-
6	5:36	5:02	4:40	-
7	6:42	4:47	-	-
8	3:40	-	-	-

the "-" sign means no action is taken

Figure 2 shows an example of normalized PPG signal over time. Data normalization will be explained in the Pre-processing section.

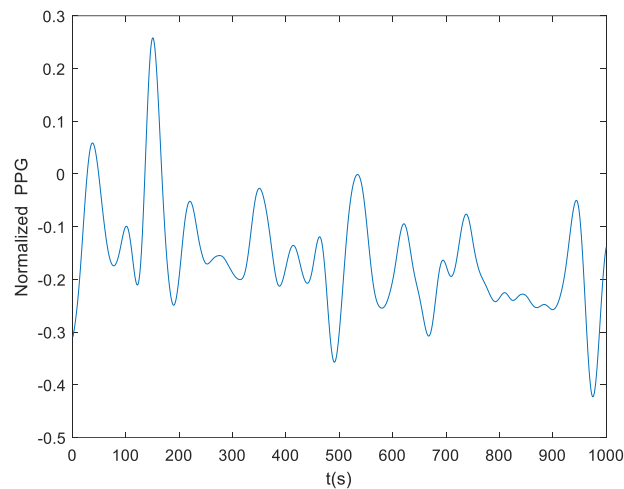


Figure 2. Changes in PPG signal over time for subject #8

Preprocessing

In this section, a second-order Butterworth filter was used to eliminate signal noise. This band-pass filter has a low cutoff frequency of 0.15 Hz and a high cutoff frequency of 15 Hz. The time series samples were then normalized using equation 1:

$$Y = 2 * (X - X_{min} / X_{max} - X_{min}) - 1 \tag{1}$$

where X represents the PPG time-series, the smallest value of the data is shown by X_{\min} , and X_{\max} symbolizes the largest value of the PPG signal. We used the windowing approach to analyze the signals. The length of the window was one second equivalent to 256 samples with no overlap.

Feature Extraction

In this experiment, the basis of the process was based on the analysis of phase space dynamics. Phase space (Poincare's plot) is a 2D representation of each sample based on the next signal sample. So, each mode of the system is displayed in phase space with a dot. One of the benefits of drawing phase space is to extract the pattern from a time series that has been moved to another dimension or space. Conventional Poincare's plots are drawn with a delay. To gain more information on the signal, some researchers suggested that the plot's higher latencies should be considered. Therefore, the delay or the " τ " in phase space can be regarded as an important parameter [17]. The concept of delay in phase space represents the number of samples in which the vertical axis based on which the sample number is drawn in the horizontal axis is " $n+\tau$ ". The resulting map, in this case, is called the "delayed Poincare's plot". Figure 3 represents a delayed PPG signal in lag of "2".

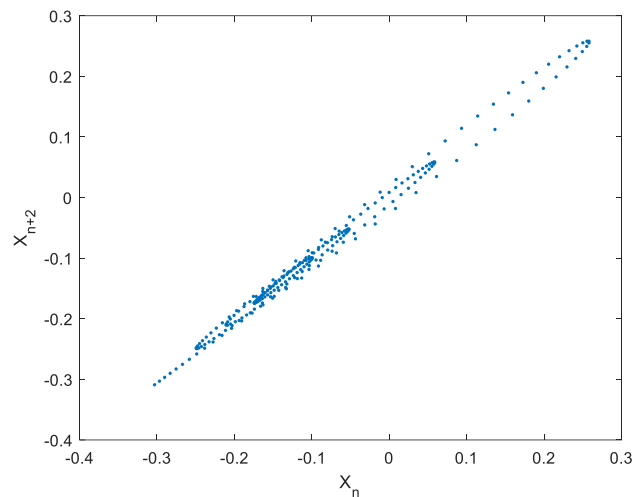


Figure 3. A Poincare's plot of PPG signal with delay of "2" for record #8

There are several ways to find the optimal delay for drawing phase space. In this paper, the mutual information method was used. In this way, information is shared between the correct selections of options for successful delays. Accordingly, the first local minimum point with the highest number of repetitions is considered the best delay [18]. In this study, the optimum delay of 10 was selected using the mutual information method.

Poincare's plots qualitatively show biological signal changes. Various methods have been proposed to quantify them [19-28]. The two conventional indices, namely SD_1 (half short oval's diameter) and SD_2 (half large oval's diameter), have been shown in Figure 4. Numerous studies have used these indices to quantify the dynamics of biological signals, especially the heart rate variability (HRV) signal [20, 29]. By plotting the phase space of the HRV signals, a mass of points is formed whose center is the mean of the signal. As a result, half the diameter of the large oval on each side will be the same for SD_2 [30]. But this is not the case in the PPG signal. In other words, the mean points are not in the center of the phase space. Consequently, the distance from the farthest point to the mean for the higher and lower samples is not the same. So, we concluded that there is some asymmetry of indices in the phase space of the PPG signal that is not observed in the cardiac signals' phase space.

Accordingly, new features of Poincaré's plots were presented in this study. For this purpose, D_1 (mean point distance to the farthest point towards the larger values of the points and along the identity line ($X_{i+\tau} = X_i$)) and D_2 (mean point distance to the farthest point towards the smaller values of the points and along the identity line) indices were considered. Also, we will evaluate the ratio of the two proposed indices (D_1/D_2) as the third feature. Figure 5 illustrates the D_1 and D_2 , schematically.

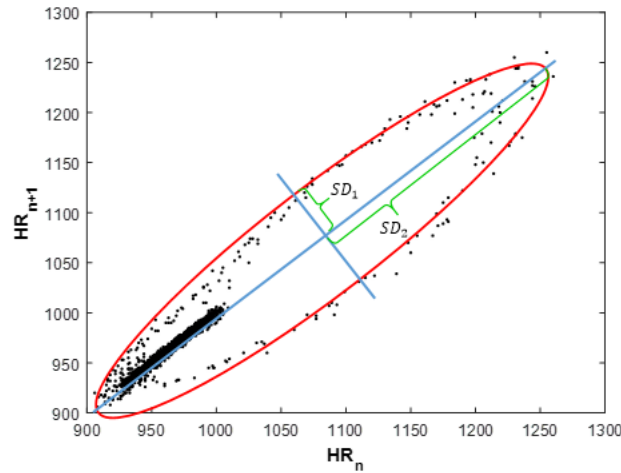


Figure 4. SD_1 and SD_2 Poincaré plot characteristics applied in the phase space of the HRV signal

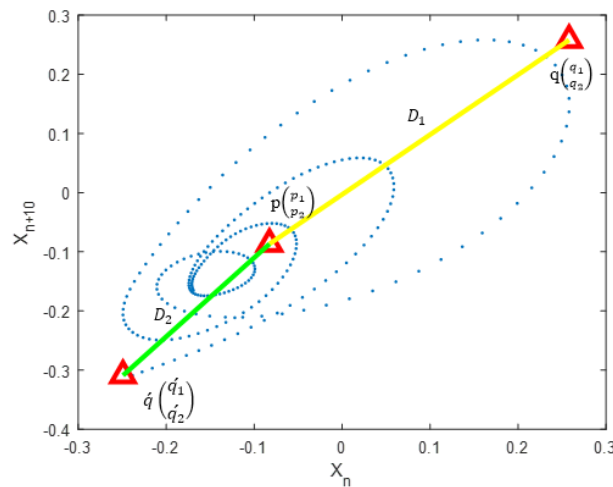


Figure 5. Phase space of a PPG signal with an optimal delay of "10" for subject # 8

The distances shown in Figure 5 were calculated using the Euclidean distance formula:

$$D_1 = \sqrt{(p_1 - q_1)^2 + (p_2 - q_2)^2} \quad (2)$$

$$D_2 = \sqrt{(p_1 + q'_1)^2 + (p_2 + q'_2)^2} \quad (3)$$

where (p_1, p_2) Cartesian coordinates of point p (mean), (q_1, q_2) Cartesian coordinates of point q (maximum) and (q'_1, q'_2) are Cartesian coordinates of point q' (minimum). To eliminate the effect of data changes in different subjects, the obtained properties (x) were normalized using the following equation:

$$x = \frac{x - \min(x)}{\max(x) - \min(x)} \quad (4)$$

where the expression $\min(x)$ denotes the property's lowest value and $\max(x)$ denotes the highest value.

Support Vector Machine Classification

The SVM classification was used to achieve the main goal, namely the classification of sports activities. This classification falls into the category of pattern recognition algorithms and operates in a supervised manner. This classifier's benefits include the simple training process, not engaging in local maximum points, the proportionality between the error rate and the complexity of the calculations. It is also possible for the user to select the kernel function. This classification was first introduced by Winnik in 1998 [31].

This classifier relocates the data to a new space called space attribute, which simplifies classification and linear separation by hyper-planes and support vectors.

In general, to classify the extraction features, the workflows are as follows:

1. Properties apply as an input to the classifier
2. Data sets are divided and labeled according to one vs all method
3. Evaluate the quality or accuracy of the training model (CrossValidation-Kfold)
4. We train the model on this set
5. We use this model to predict new data (test data)

The kernel function was the radial basis function, which is one of the most popular kernel functions.

Based on cross-validation, the K-fold method for $K=10$ was used to evaluate the classification model. The final value for K was selected after applying the values of 12,10,8,5,2 and checking the outputs of the classification. To classify the four classes, we used the one-vs-all strategy. The performance of the classifier was evaluated using accuracy, sensitivity, and specificity. The accuracy parameter value is usually expressed as a percentage and indicates the number of patterns that have been correctly identified:

$$Accuracy = (TP+TN) / (TP+FN+FP+TN) \quad (5)$$

where TP represents the number of samples that are in the first category and correctly classified in the first class; TN: Specimens belonging to the second category and correctly classified into the second category; FP: The number of samples that are in the first batch and incorrectly in the second batch; FN represents judges who are first class and wrongly classified as first class.

But another parameter, called sensitivity, is called the true positive response rate, which represents samples in the first category that belongs to the first class in the classification and is calculated from equation 6:

$$Sensitivity (TPR) = TP / (TP+FN) \quad (6)$$

Another parameter to be considered for this classification is specificity, which represents the rate of true negative responses. That is, the data for the second category are correctly assigned to the second category:

$$Specificity (TNR) = TN / (TN+FP) \quad (7)$$

Statistical Analysis

The Wilcoxon rank sum test was used to evaluate the similarity between the two groups on the feature space (D1, D2, D1/D2) and to show the degree of difference between them. It is a relatively robust test that examines both the direction and extent of change. Using the rank-sum syntax in MATLAB, we investigate the null hypothesis about two sets of data. This test is based on the assumption that the two groups have an equal mean. However, they could have unequal lengths. According to the index (p-value), if this value is less than 0.05, the difference between the groups is not random.

Results

To evaluate the analysis performed, a diagram of the changes in all three properties (D1, D2, D1/D2) for different exercise activities is shown in Figure 6.

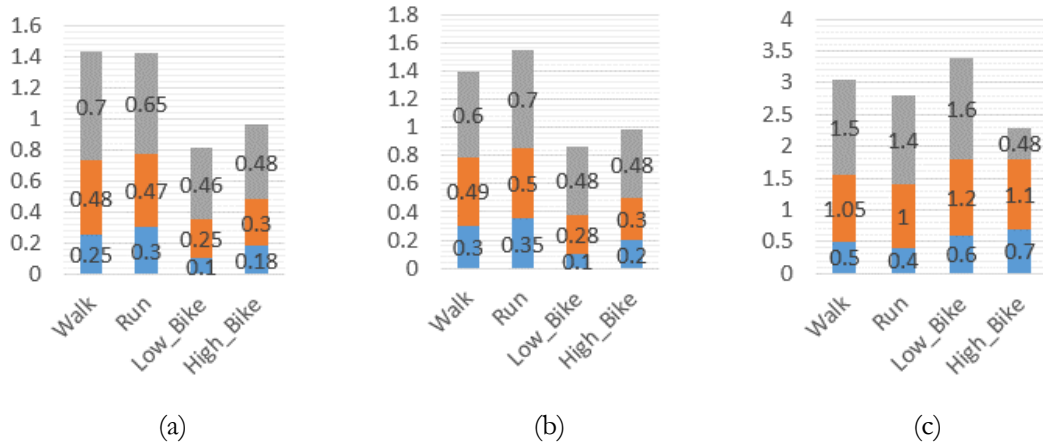


Figure 6. Variations in the features for walking, running, low and high cycling; (a) D1, (b) D2, and (c) D1/ D2 (Note – Orange: Average; Gray: The variance after mean; Blue: Pre-mean variance). The vertical axis demonstrates the D1, D2, and D1/D2 values in (a), (b), and (c) respectively, and the horizontal axis shows the sport state activity

The highest mean value of D1 is 0.48, which is obtained for walking. The second greater value of D1 is 0.47 for running activity. In contrast, the largest values of D2 are 0.5 and 0.49 during running and walking respectively. According to Figure 6, the lowest mean value and the lowest range of changes in the D1 and D2 are related to low resistance cycling. In addition, the highest amount of variance for D1 and D2 indicators is obtained in these two physical activities, i.e. running and walking. Nevertheless, D1/D2 has the highest mean and variations for all physical activity.

The values of D1 and D2 in both running and walking are higher than that of biking (low and high resistance). Therefore, performing these two sports has caused the expansion of the points in the phase space.

Using the Wilcoxon test, significant differences between various activities were examined, and the results are shown in Table 2.

Table 2. Wilcoxon results: p-values

State Feature	W vs R	W vs H-B	W vs L-B	R vs H-B	R vs L-B	L-B vs H-B
D ₁	0.1	5.01×10 ⁻¹⁹²	0	3.94×10 ⁻²⁰⁵	0	2.23×10 ⁻⁹⁶
D ₂	1.5×10 ⁻³⁰	1.41×10 ⁻²⁸⁷	0	0	0	4.35×10 ⁻⁸⁹
D ₁ /D ₂	6.92×10 ²¹	1.29×10 ⁻⁴	2.32×10 ⁻⁸	2.61×10 ⁻³²	1.7×10 ⁻⁴⁷	0.3

Note- W: Walk, R: Run, L-B: Low-resistance Bicycle, H-B: High-resistance bicycle.

According to the results of Table 2, there was a significant difference (p < 0.05) between all sport modes, except for between the "walk and run" mode for the D1 feature and between the "light and heavy cycling" for the D1/D2 feature. Finally, by applying the support vector machine classification, the activities of walking, running, light and heavy cycling were detected. Table 3 shows the results.

According to the results of Table 3, the highest classification accuracy was related to high resistance bicycle activity. In this case, the mean accuracy is 83.52%. It also has the highest sensitivity parameter with a rate of 84%. However, its specificity is the minimum one. The walking mode achieved the second-best accuracy rate. It has the maximum specificity and second score of sensitivity

values. Precisely, the mean accuracy, specificity, and sensitivity rates are 80.17, 75, and 81%, respectively. The lowest accuracy and sensitivity rates are obtained for discriminating running mode.

Table 3. SVM classification results

Activity	Metric name	Value (%)
Walk vs the other states*	Accuracy	80.17±27.73
	Specificity	75±1
	Sensitivity	81±0.0447
Run vs the other states	Accuracy	78.17±27.69
	Specificity	64±0.71
	Sensitivity	80±0.45
High Resistance Bicycle vs the * other states	Accuracy	83.52±0.76
	Specificity	36±1.04
	Sensitivity	84±0.4
Low Resistance Bicycle vs the other states	Accuracy	78.46±29.39
	Specificity	64±0.84
	Sensitivity	80±0.55

Discussion

Our study showed that by doing exercise effort, the phase space's geometry and consequently the dynamics of the PPG signal changes significantly. To the best of our knowledge, it is the first study to use the state space approach to investigate finger PPG waves' dynamics during physical exercise. Former studies have mainly focused on the time and spectral characteristics of cardiac signals. Their results revealed that physical efforts prompt an overall reduction in HRV. Moreover, on account of the physical activity, a drop in total/HF power and a constant/diminished LF power are found, related to higher sympathetic activity and a lower parasympathetic activity [9, 37, 38]. According to [36], significant changes of PPG signal with sharp peaks were observed during exercise. These changes reflect the effect of exercise on the cardiovascular and respiratory systems, which, over time, with proper monitoring, results in strength training. The advantage of the proposed measures over the traditional methods is that no need to make a stationary assumption for the analyzed signal, which is the case for traditional techniques. Additionally, easy interpretation and simplicity allow it to be used on portable devices such as Holters. Our results also showed that the type of physical activity affects the PPG dynamics. For comparison, however, we did not find a study that examined the effect of several types of exercise on PPG/cardiac signals. This experiment has also highlighted the usefulness of simple proposed features in quantifying the asymmetry in the signals' phase space. Previously, some efforts have been made to quantify PPG phase space's shape [22, 26].

On the other hand, some algorithms have been proposed to quantify the HRV-signal asymmetry [39-42]. However, no attention has been paid to the PPG-signal and changes in its asymmetry. Moreover, in this study, the approach of classifying PPG characteristics in different exercises was adopted. Acceptable accuracy rates were obtained for physical activity classification. For comparison, Table 4 provides the results of the studies conducted in the last 4 years and examines the methodology used in this study.

The results of studies in Table 4 show that by using features such as mean and standard deviation, some studies have achieved a high classification percentage. In the present study, due to the new extractive features and the existence of four classification classes, we achieved a separation percentage of over 80%. Also, like the statistical analysis section of Table 4, we were able to detect a significant difference between the sports activities. According to [36], the significant changes of PPG signal with sharp peaks were observed during exercise. These changes reflect the effect of exercise on the cardiovascular and respiratory systems, which, over time, with proper monitoring, results in strength training. Also, based on the performance of the classification, the proposed scheme can be used to

improve individual planning in the field of sports and health. These new indices can be used to design people's physical activity planning programs.

Table 4. Review of recent studies in signal processing and classification of sports activities

Ref	Year	Data	Method	Result
[2]	2018	25 Healthy male adults age = 28.1±3.8 (years)	1. HR Signal 2. Segmentation (13 s) 3. Feature extraction: mean and standard deviation 4. Classification: Random Forest	1. Overall Accuracy for varying intensities of cycling.: 89.4±4.2%
[33]	2018	2 Test users of 22 years' old: Male And Female	1. ECG and PPG Signal in: Squats, Dumbbell curl, Walking, Jumping, Pushups, Jumping-jacks 2. Feature Extraction: mean, standard deviation and median Signals 3. Activity Recognition	1. during physical activities, measurements had sudden variations in HR with a delay, due to movements of the wrist 2. by combining HR monitoring and activity recognition, personal suggestions for physical activities are generated using a tag-based recommender and rule-based filter
[34]	2019	12 Subjects	1. PPG signal 2. Preprocessing 3. Tracking 4. Classification: KNN Classifier	1. Classification between high-intensity and low-intensity physical activities, 2. improve the tracking accuracy
[35]	2018	15 Cyclists	1. PPG signal 2. Signal preprocessing 3. HR feature extraction by using the Karvonen formula: Reserve HR, target HR, rHR 4. Regression Analysis and Discriminant Analysis	1. Discriminant analysis was 88.3% successfully classified cyclist into 3 group of trained and untrained cyclist
[36]	2016	TROIKA dataset: 12 male subjects with ages ranging from 18 to 35	1. ECG and PPG Signal 2. Preprocessing 3. Clustering sources using Partition Around Medoids 4. Unsupervised Training using Restricted Boltzman Machines 5. Supervised Training of Deep Belief Networks	1. this technique is robust against motion induced noise and thus suitable for usage in day to day settings 2. this procedure can be extended to build personalized models for clinical metrics calculation like HR, blood pressure using PPG signals in uncontrolled environments
This Study	2020	Physionet Dataset: Wrist PPG during Exercise	1. PPG signal in 4 state of physical activity: walk, run, Low resistance bicycle, High resistance bicycle 2. Preprocessing 3. Phase Space 4. Delay Poincare Plot 5. Feature Extraction: D_1 , D_2 , D_1/D_2 6. Wilcoxon test ($p < 0.05$) 7. Classification: SVM	1. Introducing new features: D_1 , D_2 , D_1/D_2 2. Significant difference between 4 state of physical activity 3. Classification Accuracy: 83.52% for High resistance bicycle 80.17% for Walk state

It should be noted that this study also has some limitations. The present study used the available signals at the Physionet database [16]. This database includes a limited number of participants whose medical condition is unclear. Thus, there are too few signals to draw correct conclusions. Upcoming work should involve a larger number of participants so that the proposed algorithm can be accurately validated. The body's response to the physical effort will always be different depending on age, training, associated pathologies. On the other hand, the database does not provide any information about the participants' sports skills. However, former works have stressed that a higher HRV and parasympathetic activity is obtained by endurance training, while at rest, the sympathetic activity has diminished [9, 43]. Additionally, endurance-trained participants unveil a greater parasympathetic activity compared to the untrained controls [43]. In future work, the proposed algorithm should be considered in groups with different levels of physical fitness. In this study, the phase space asymmetry of PPG signals along the identity line, similar to the SD2 index in the cardiac phase space, was investigated. For future works, we can examine similar asymmetry for the plot in the direction perpendicular to the identity line. Other classifiers should also be examined to improve the performance of sports mode detection.

Conclusion

The proposed method has some advantages, such as a low-computational cost, simplicity, and resulted in a high percentage of accuracy and classification sensitivity. Using the support vector machine we achieved a classification accuracy of 83.52% for heavy cycling mode and 80.17% for walking mode.

Ethical Issues

This article examined the PPG signals of Physionet dataset [16], which is freely available in the public domain.

Conflict of Interest

The authors declare that they have no conflict of interest.

References

1. Ghasemnejad DA. The Role of Exercise in Mental Health. *Neshate Varzesh* 2007; 7: 7-10 (Text in Persian).
2. Mehrang S, Pietilä J, Korhonen I. An activity recognition framework deploying the random forest classifier and a single optical heart rate monitoring and triaxial accelerometer wrist-band. *Sensors* 2018;18(2):613.
3. Hosseini M, Piri M, Agha Alinejad H. The Effect of Endurance, Strength, and Parallel Exercises on Cardiac Performance in College Girls. *Olympic* 2011; 1(49): 117-126. (Text in Persian).
4. Piralaiy E, Siahkuhian M, Nikokheslat S, Bolboli L, Abadi NA, Sheikhalizadeh M, et al. Efficacy of the Moderate Intensity Aerobic training on Heart Rate Variability (HRV) in Patients with the Type-2 Diabetic Neuropathy. *Majallah-i pizishki-i Danishgah-i Ulum-i Pizishki va Khadamat-i Bihdashti-i Darmani-i Tabriz*. 2019;41(3):44-52.
5. Keihani D, Kargarfard M, Mokhtari M. Cardiac effects of exercise rehabilitation on quality of life, depression and anxiety in patients with heart failure patients. *Journal of Fundamentals of Mental Health* 2014;17(1):13-9.

6. Shirzadi E, Sarfehju K, Esmaeilvandi I, Abedi M. The effect of Exercise on Human Physical and Mental Health. 5th Iranian Scientific Conference on Educational and Psychological Sciences. 2017. Tehran, Iran. (Text in Persian).
7. Rostami N, Ghasemzadeh S, Sanambar M. Exercise and Heart Disease. First National Conference on Advances and Challenges in Scienc. 2015. Shiraz, Iran. (Text in Persian)
8. Ahmed MU, Loutfi A. Physical activity identification using supervised machine learning and based on pulse rate. International Journal of Advanced Computer Sciences and Applications 2013;4(7):210-7.
9. Carter JB, Banister EW, Blaber AP. Effect of Endurance Exercise on Autonomic Control of Heart Rate. Sports Med 2003;33:33-46.
10. Lewis MJ, Short AL. Differences in QT interval determined from multi-lead ambulatory ECG during rest and physical exercise. Biomedical Signal Processing and Control 2006, pp. 219-28.
11. Lai E, Boyd K, Albert D, Ciocca M, Chung EH. Heart rate variability in concussed athletes: A case report using the smartphone electrocardiogram. HeartRhythm Case Rep. 2017;3(11):523-6.
12. Ciucurel C, Georgescu L, Iconaru EI. ECG response to submaximal exercise from the perspective of Golden Ratio harmonic rhythm. Biomedical Signal Processing and Control 2018;40:159-62.
13. Wang A, Yang L, Wen W, Zhang S, Gu G, Zheng D. Gaussian modelling characteristics changes derived from finger photoplethysmographic pulses during exercise and recovery. Microvascular Research 2018;116:20-5.
14. Kuppusamy M, Kamaldeen D, Pitani R, Amaldas J, Ramasamy P, Shanmugam P, et al. Effects of yoga breathing practice on heart rate variability in healthy adolescents: a randomized controlled trial. Integr Med Res. 2020;9(1):28-32.
15. Islam MT, Zabir I, Ahamed T, Yasar T, Shahnaz C, Fattah SA. A time-frequency domain approach of heart rate estimation from photoplethysmographic (PPG) signal. Biomedical Signal Processing and Control 2017;36:146-54.
16. Jarchi D, Casson AJ. Description of a database containing wrist PPG signals recorded during physical exercise with both accelerometer and gyroscope measures of motion. Data 2017;2(1):1. doi: 10.3390/data2010001
17. Nejadgholi I, Moradi MH, Abdolali F. Using phase space reconstruction for patient independent heartbeat classification in comparison with some benchmark methods. Computers in Biology and Medicine 2011;41(6):411-9.
18. Kantz H, Schreiber T. Nonlinear time series analysis: Cambridge University Press; 2004.
19. Yang S. Nonlinear signal classification in the framework of high-dimensional shape analysis in reconstructed state space. IEEE Trans Circuits Syst II Express Briefs 2005;52:512-6.
20. Luo C, Li Q, Rao H, Huang X, Jiang H, Rao N. An improved Poincaré plot-based method to detect atrial fibrillation from short single-lead ECG. Biomedical Signal Processing and Control 2021;64:102264.
21. Goshvarpour A, Goshvarpour A. Poincare indices for analyzing meditative heart rate signals. Biomed J. 2015;38(3):229-34.
22. Goshvarpour A, Goshvarpour A. Poincaré's section analysis for PPG-based automatic emotion recognition. Chaos, Solitons & Fractals 2018;114:400-7.
23. Goshvarpour A, Goshvarpour A. Do meditators and non-meditators have different HRV dynamics? Cognitive Systems Research 2019;54:21-36.
24. Goshvarpour A, Goshvarpour A. Gender and age classification using a new Poincare section-based feature set of ECG. Signal, Image and Video Processing 2019;13(3):531-9.
25. Goshvarpour A, Goshvarpour A. A novel approach for EEG electrode selection in automated emotion recognition based on Lagged Poincaré's Indices and sLORETA. Cognitive Computation. 2020;12(3):602-18.
26. Goshvarpour A, Goshvarpour A. Asymmetry of lagged Poincare plot in heart rate signals during meditation. Journal of Traditional and Complementary Medicine 2021;11(1):16-21.
27. Yan C, Li P, Liu C, Wang X, Yin C, Yao L. Novel gridded descriptors of poincaré plot for analyzing heartbeat interval time-series. Computers in Biology and Medicine 2019;109:280-9.

28. Goshvarpour A, Goshvarpour A, Rahati S. Analysis of lagged Poincare plots in heart rate signals during meditation. *Digital Signal Processing* 2011;21(2):208-14.
29. Massaro S, Pecchia L. Heart rate variability (HRV) analysis: A methodology for organizational neuroscience. *Organizational Research Methods* 2019;22(1):354-93.
30. Constantinescu V, Matei D, Costache V, Cuciureanu D, Arsenescu-Georgescu C. Linear and nonlinear parameters of heart rate variability in ischemic stroke patients. *Neurologia i Neurochirurgia Polska* 2018;52(2):194-206.
31. Burger C (Ed). *A Tutorial on Support Vector Machines for Pattern Recognition, Data Mining And Knowledge Discovery* 1998: Workshop On Data Mining And Knowledge Discovery.
32. Casson AJ. [Internet] 2017. Available from: <https://physionet.org/files/wrist/1.0.0/>.
33. De Pessemier T, Martens L. Heart rate monitoring, activity recognition, and recommendation for e-coaching. *Multimedia Tools and Applications* 2018;77(18):23317-34.
34. Biagetti G, Crippa P, Falaschetti L, Orcioni S, Turchetti C. Reduced complexity algorithm for heart rate monitoring from PPG signals using automatic activity intensity classifier. *Biomedical Signal Processing and Control* 2019;52:293-301.
35. Sudin S, Shakaff A, Zakaria A, Salleh A, Saad F, Abdullah A. Cyclist Performance Classification System based on Submaximal Fitness Test. *Journal of Telecommunication, Electronic and Computer Engineering (JTEC)*. 2018;10(1-13):73-8.
36. Jindal V, Birjandtalab J, Pouyan MB, Nourani M, editors. An adaptive deep learning approach for PPG-based identification. 2016 38th Annual international conference of the IEEE engineering in medicine and biology society (EMBC); 2016: IEEE.
37. Gall B, Parkhouse W, Goodman D. Heart rate variability of recently concussed athletes at rest and exercise. *Med Sci Sports Exerc* 2004;36:1269-74.
38. James DVB, Barnes AJ, Lopes P, DM W. Heart rate variability: response following a single bout of interval training. *Int J Sport Med* 2002;44:247_51.
39. Atefeh Goshvarpour, Ateke Goshvarpour. Asymmetry of lagged Poincare plot in heart rate signals during meditation. *Journal of Traditional and Complementary Medicine*. 2021;11(1):16-21.
40. Alvarez-Ramirez J, Echeverria JC, Meraz M, Rodriguez E. Asymmetric acceleration/deceleration dynamics in heart rate variability. *Physica A* 2017;479:213-24.
41. Jiang J, Chen X, Zhang C, Wang G, Fang J, Ma J, Zhang J. Heart rate acceleration runs and deceleration runs in patients with obstructive sleep apnea syndrome. *Sleep Breath*. 2017;21(2):443-51.
42. Yan C, Li P, Ji L, Yao L, Karmakar C, Liu C. Area asymmetry of heart rate variability signal. *Biomed Eng Online*. 2017;16(1):112.
43. Goldsmith R, Bloomfeld DM, Rosenwinkel ET. Exercise and autonomic function. *Coron. Artery Dis*. 2000;11:129-35.